Superconducting quantum interference devices with different damped junctions operated in directly coupled current- and voltage-bias modes*

Zeng Jia(曾 佳)[a)b)c)d)], Zhang Yi(张 懿)[b)c)], Qiu Yang(邱 阳)[a)c)d)], Zhang Guo-Feng(张国峰)[a)c)], Wang Yong-Liang(王永良)[a)c)], Kong Xiang-Yan(孔祥燕)[a)c)†], and Xie Xiao-Ming(谢晓明)[a)c)]

[a)] *State Key Laboratory of Functional Materials for Informatics, Shanghai Institute of Microsystem and Information Technology, Chinese Academy of Sciences, Shanghai* 200050, *China*

[b)] *Peter Grünberg Institute (PGI-8), Forschungszentrum Jülich (FZJ), D-52425 Jülich, Germany*

[c)] *Joint Research Laboratory on Superconductivity and Bioelectronics, Collaboration between CAS-Shanghai, Shanghai* 200050, *China and FZJ, D-52425 Jülich Germany*

[d)] *University of Chinese Academy of Sciences, Beijing* 100049, *China*

(Received 6 March 2014; revised manuscript received 3 June 2014; published online 24 September 2014)

We investigate niobium thin film superconducting quantum interference devices (SQUIDs) with different Steward–McCumber parameters β_c operated in both current- and voltage-bias modes. We experimentally prove that there is no difference between the two bias modes with respect to the SQUID intrinsic noise and the noise contribution from the preamplifier. Furthermore, the relationships of the SQUID dynamic parameters, $(R_d)_{\text{current bias}} \approx (R_d)_{\text{voltage bias}}$ and $(\partial V/\partial \Phi)_{\text{current bias}} \approx [(\partial i/\partial \Phi)R_d]_{\text{voltage bias}}$, are always satisfied. For a strongly damped SQUID with $\beta_c \approx 0.25$, additional positive feedback (APF) and noise cancellation (NC) were employed to enhance $\partial V/\partial \Phi$, the former showing a degradation in the linear flux range but otherwise the same with NC. For a weakly damped SQUID with $\beta_c \approx 3$, it is directly connected to the preamplifier without APF or NC, and a low SQUID system noise of about 4 $\mu\Phi_0/\sqrt{\text{Hz}}$ is measured, which is close to its intrinsic noise.

Keywords: SQUID, noise, bias mode, Steward–McCumber parameter

PACS: 85.25.Dq, 43.50.+y, 85.25.Hv **DOI:** 10.1088/1674-1056/23/11/118501

1. Introduction

Generally, there are two bias modes in the SQUID readout schemes, namely, the current-bias mode and the voltage-bias mode. With respect to the intrinsic noise $\delta\Phi_s$ and noise contribution $\delta\Phi_{\text{preamp}}$ from the preamplifier, there is no difference between the two bias modes.[1]

In the current-bias mode, the SQUID was traditionally operated in the flux modulation scheme (FMS)[2] or the direct readout scheme (DRS) with additional positive feedback (APF)[3] to suppress $\delta\Phi_{\text{preamp}}$. In the voltage-bias mode, noise cancellation (NC)[4] and SQUID bootstrap circuitry (SBC)[5] were introduced in DRS as an alternative way. Usually, biasing the SQUID under the voltage and read it out by a second SQUID will yield the lowest preamplifier noise.[6,7]

Recently, our research has shown that weakly damped SQUIDs with large β_c $(= 2\pi I_c C R_J^2/\Phi > 1)$ exhibit a large flux-to-voltage transfer coefficient $\partial V/\partial \Phi$ without experiencing instabilities.[8,9] Here, I_c denotes the critical current per junction, C its self-capacitance, R_J the junction shunt resistance, and Φ the magnetic flux quantum. In this case, the SQUID can be directly connected to an operational amplifier without any additional feedback circuitry to reduce $\delta\Phi_{\text{preamp}}$.[10,11] DRS has become more and more popular in the last few decades, stimulated in part by the need of its higher bandwidth and slew rate compared with FMS.

In this work, the helium-cooled niobium dc SQUIDs with different β_c are employed and the same one preamplifier in our DRS for both current-and voltage bias modes is utilized. We measured the SQUID parameters such as $\partial V/\partial \Phi$, $\partial i/\partial \Phi$ (flux-to-current transfer coefficient), R_d (SQUID dynamic resistance) and the SQUID system noise $\delta\Phi$ to experimentally study the similarities and differences between the two bias modes. The comparison of SQUID parameters and characteristics between APF and NC for the strongly damped SQUID is also demonstrated.

2. Experimental setup

Figure 1 shows the schematic circuit diagram for the SQUID measurements. OP-1 represents the preamplifier with a non-inverting amplification factor (AF) of R_2/R_1 $(R_2 \gg R_1)$. When K_1 and K_2 are in position 1, the SQUID is operated in current-bias mode with a bias-current of V_b/R_b $(R_b \gg R_d)$ flowing through the SQUID. In this case, OP-2 is an inverting operational amplifier with the AF of $-R_{I2}/R_{I1}$, resulting

*Project supported by the Strategic Priority Research Program (B) of the Chinese Academy of Sciences (Grant No. XDB04010100) and One Hundred Person Project of the Chinese Academy of Sciences.

†Corresponding author. E-mail: xykong@mail.sim.ac.cn

© 2014 Chinese Physical Society and IOP Publishing Ltd

in a total voltage AF of $-(R_2R_{I2})/(R_1R_{I1})$ combined with OP-1. When K_1 and K_2 are in position 2, the SQUID is voltage-biased with the bias voltage of $(V_bR_{V1}/R_{V2})/(R_2/R_1)$ ($R_{V2} \gg R_{V1}$). Here, OP-1 and OP-2 actually act as a current-to-voltage convertor with a gain of R_b.

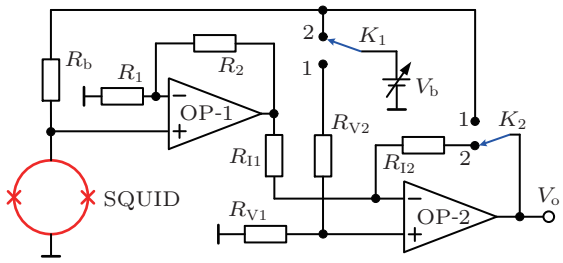


Fig. 1. (color online) Schematic circuit diagram for current-and voltage-bias modes using the same preamplifier OP-1. K_1 and K_2 switch synchronously: position 1 represents the current-bias mode while position 2 the voltage-bias mode.

Planar niobium-SQUID magnetometers with a chip size of 5×5 mm^2 and a SQUID inductance of $L_s = 350$ pH were employed. The flux-to-field transfer coefficient $\partial B/\partial\Phi$ was measured to be 1.5 nT/Φ_0. The voltage feedback circuit consisting of an inductor and a resistor in series was also integrated for both APF and NC operation. For more information about the layout of the magnetometer, the reader can refer to.[12] All SQUID chips were placed in a niobium shielding tube to perform the measurements including their noise spectrum measured in a flux-locked loop (FLL).

We obtained a nominal β_c by the measured I_c, the measured R_J from the I–V characteristics at large bias current and an estimated $C \approx 360$ fF from the junction's geometry. To get a wide range of β_c, R_J was varied while keeping I_c and C constant.

3. SQUID measurements

3.1. Measurements of the strongly damped SQUID ($\beta_c \approx 0.25$)

Figure 2 exhibits the measurements of a strongly damped SQUID with $\beta_c \approx 0.25$ ($2I_c \approx 8$ μA, $R_J \approx 7.5$ Ω). In current-bias mode, the noise-rounded V–Φ curve without APF (Fig. 2(a)) is quasi-sinusoidal and symmetric. APF steepened the shape in one slope with a somewhat reduced voltage swing V_{swing} (Fig. 2(b)). Indeed, when APF is employed, both $\partial V/\partial\Phi$ and R_d at the working point W are further improved from 87 μV/Φ_0 to 715 μV/Φ_0 and 7.8 Ω to 81 Ω, respectively. In voltage-bias mode, the shapes of the I–Φ curves without (Fig. 2(c)) and with (Fig. 2(d)) NC are almost the same, resulting in an unchanged $\partial i/\partial\Phi \approx 9.5$ μA/Φ_0. However, NC makes a marked increase of R_d at W from 8.7 Ω to 78 Ω, thus leading to a further increase of $(\partial i/\partial\Phi)\cdot R_d$ from 85 μV/Φ_0 to 725 μV/Φ_0. It is obvious that no matter whether APF or NC is introduced or not, the relationships, $(R_d)_{\text{current bias}} \approx (R_d)_{\text{voltage bias}}$ and $(\partial V/\partial\Phi)_{\text{current bias}} \approx ((\partial i/\partial\Phi)\cdot R_d)_{\text{voltage bias}}$, are always satisfied.

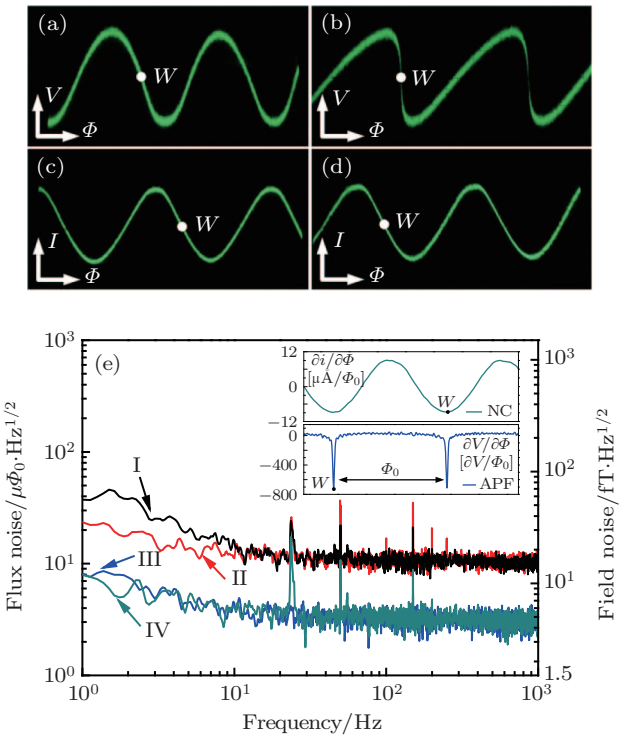


Fig. 2. (color online) Measurements of SQUID with $\beta_c \approx 0.25$: V–Φ curve in current-bias mode without APF (a); with APF (b); I–Φ curve in voltage-bias mode without NC (c); with NC (d). (e) shows the noise measurement. The inset shows the derivatives of (b) and (d).

The measured SQUID system noise $\delta\Phi$, which is the sum of $\delta\Phi_s$ and $\delta\Phi_{preamp}$, i.e., $\delta\Phi = [\delta\Phi_s^2 + \delta\Phi_{preamp}^2]^{1/2}$ is shown in Fig. 2(e). In our DRS, a commercial operational amplifier (AD797) with a voltage noise $V_n \approx 0.9$ nV/$\sqrt{\text{Hz}}$ (> 100 Hz) was used as the preamplifier, whose noise contribution can be expressed as $\delta\Phi_{preamp} \approx V_n/(\partial V/\partial\Phi)$. Curve I and II were measured at W in Figs. 2(a) and 2(c), respectively. Here, the SQUID system noise $\delta\Phi$ is the same between the two bias modes and is dominated by the preamplifier noise contribution, i.e., $\delta\Phi \approx \delta\Phi_{preamp} = V_n/(\partial V/\partial\Phi) \approx 10.6\ \mu\Phi_0/\sqrt{\text{Hz}}$, due to the same small $\partial V/\partial\Phi$ of about 85 μV/Φ_0. Curve III and IV were measured at W in Figs. 2(b) and 2(d) showing a much suppressed $\delta\Phi \approx 3\ \mu\Phi_0/\sqrt{\text{Hz}}$ with the field noise $\delta B \approx 4.5$ fT/$\sqrt{\text{Hz}}$ due to the enhanced $\partial V/\partial\Phi$ to about 720 μV/Φ_0. In this case, $\delta\Phi_{preamp}$ is reduced to 1.25 $\mu\Phi_0/\sqrt{\text{Hz}}$ resulting in a derived $\delta\Phi_s \approx 2.7\ \mu\Phi_0/\sqrt{\text{Hz}}$.

It is concluded from curve I–IV that there is, in principle, no difference between the two-bias modes (no matter whether APF or NC is employed or not) with respect to the SQUID intrinsic noise and the noise contribution from the preamplifier.[1,13] For meaningful statistics, we measured about 300 SQUID magnetometers with both bias modes to support this result. However, compared with NC, APF de-

grades the linear flux range, as shown in the inset in Fig. 2(e), thus possibly reducing the system slew rate.[1]

All the parameters of this strongly damped SQUID measured by the two bias modes both with and without APF or NC are summarized in Table 1.

Table 1. Parameters of the SQUID with $\beta_c \approx 0.25$ measured in both current- and voltage-bias modes.

Bias mode	Current-bias mode		Voltage-bias mode	
	without APF	with APF	without NC	with NC
$V_{swing}^{a)}/\mu V$	22	18	/	/
$I_{swing}^{b)}/\mu A$	/	/	2.7	2.7
$\partial V/\partial \Phi^{a)}/(\mu V/\Phi_0)$	87	715	85[g)]	725[g)]
$\partial i/\partial \Phi^{b)}/(\mu A/\Phi_0)$	/	/	9.6	9.3
$R_d^{c)}/\Omega$	7.8	81.6	8.7	78
$\delta\Phi^{d)}/(\mu\Phi_0/\sqrt{Hz})$	10.6	3	10.6	3
$\delta\Phi_{preamp}^{e)}/(\mu\Phi_0/\sqrt{Hz})$	10.4	1.26	10.6	1.24
$\delta\Phi_s^{f)}/(\mu\Phi_0/\sqrt{Hz})$	...[h)]	2.7	...[h)]	2.7

[a)] Measured from the V–Φ curve.

[b)] Measured from the I–Φ curve.

[c)] Derived from the I–V characteristics.

[d)] Measured SQUID system noise (see Fig. 2(e)).

[e)] Calculated by $\delta\Phi_{preamp} = V_n/(\partial V/\partial\Phi)$.

[f)] Derived by $\delta\Phi_s = (\delta\Phi^2\delta\Phi_{preamp}^2)^{1/2}$. [g)] $\partial V/\partial\Phi = (\partial i/\partial\Phi)R_d$.

[h)] Not determined.

3.2. Measurements of the weakly damped SQUID ($\beta_c \approx 3$)

Recently, SQUIDs with weakly damped junctions have attracted a lot of attention.[8] In this case, the SQUIDs can be read out directly by a commercial operational amplifier without the need for additional feedback circuitries to suppress the preamplifier noise, thus simplifying the SQUID system substantially.[10,11] However, it is confirmed both by simulations[14,15] and experiments[9] that the intrinsic noise $\delta\Phi_s$ increases with increasing β_c.

Figure 3 shows the noise measurements of the SQUID with $\beta_c \approx 3$ (here, $2I_c \approx 9.5$ μA, $R_J \approx 23$ Ω) in DRS without an additional feedback circuit. The SQUID system noise spectra measured in current-bias mode (Curve I) and voltage-bias mode (Curve II) exhibit an extreme consistency with $\delta\Phi \approx 4\ \mu\Phi_0/\sqrt{Hz}$ and $\delta B \approx 6$ fT/$\sqrt{Hz}$. It once again proves that there is no difference between the two bias modes regarding the noise. The inset shows the V–Φ and I–Φ characteristics with $(R_d)_{current\ bias} \approx (R_d)_{voltage\ bias} = 50\ \Omega$ and $(\partial V/\partial\Phi)_{current\ bias} \approx ((\partial i/\partial\Phi)R_d)_{voltage\ bias} = 440\ \mu V/\Phi_0$ obtained at the working point W. In this case, the preamplifier noise contribution can be derived to be $\delta\Phi_{preamp} = V_n/(\partial V/\partial\Phi) = (0.9\ nV/\sqrt{Hz})/(440\ \mu V/\Phi_0) \approx 2\ \mu\Phi_0/\sqrt{Hz}$. By subtracting $\delta\Phi_{preamp}$ from the measured $\delta\Phi$, $\delta\Phi_s \approx 3.5\ \mu\Phi_0/\sqrt{Hz}$ is obtained, which is confirmed by measuring the noise again (Curve III) with an ultra low noise preamplifier (ULNP) with a voltage noise $V_n \approx 0.37$ nV/$\sqrt{Hz}$ (> 2 Hz).[9]

All the parameters of this weakly damped SQUID measured by two bias modes without additional feedback circuitries are summarized in Table 2. Compared with the strongly damped SQUID ($\beta_c \approx 0.25$) measured with APF or NC, the weakly damped SQUID with $\beta_c \approx 3$ only exhibits an increase of about 30% for the measured system noise, which is sufficient to meet a lot of practical applications. Due to the convenience of simple readout, the weakly damped SQUID is a very promising choice to construct a multi-channel SQUID system.

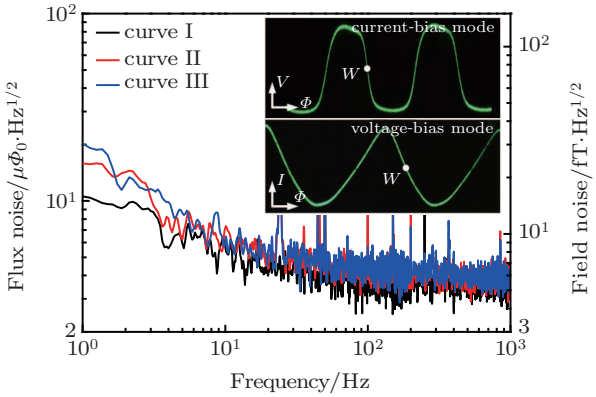


Fig. 3. (color online) Noise characteristics of the SQUID with $\beta_c \approx 3$. The inset shows the photos of V–Φ and I–Φ curves, respectively. W denotes the working point.

Table 2. Parameters of the SQUID with $\beta_c \approx 3$ measured by both current- and voltage-bias modes.

	Current-bias mode	Voltage-bias mode
$V_{swing}/\mu V$	50	/
$I_{swing}/\mu A$	/	2.2
$\partial V/\partial\Phi/(\mu V/\Phi_0)$	450	435
$\partial i/\partial\Phi/(\mu A/\Phi_0)$	/	8.7
R_d/Ω	50	50
$\delta\Phi/(\mu\Phi_0/\sqrt{Hz})$	4	4
$\delta\Phi_{preamp}/(\mu\Phi_0/\sqrt{Hz})$	2	2
$\delta\Phi_s/(\mu\Phi_0/\sqrt{Hz})$	3.5	3.5

4. Conclusion

To conclude, we demonstrated the behavior of SQUIDs with different β_c operated in both current- and voltage-bias modes. It was experimentally proved that there was no difference between the two bias modes with respect to the SQUID intrinsic noise and the noise contribution from the preamplifier. Furthermore, the relationships, $(R_d)_{current\ bias} \approx (R_d)_{voltage\ bias}$ and $(\partial V/\partial\Phi)_{current\ bias} \approx ((\partial i/\partial\Phi)R_d)_{voltage\ bias}$, were always satisfied.

For the strongly damped SQUID with $\beta_c \approx 0.25$, APF and NC were introduced to suppress the preamplifier noise, leading to a measured SQUID system noise $\delta\Phi$ of about $3\mu\Phi_0/\sqrt{Hz}$. Compared with NC, APF degraded the linear flux range a great deal, thus reducing the slew rate. For the weakly damped SQUID with $\beta_c \approx 3$, $\delta\Phi \approx 4\ \mu\Phi_0/\sqrt{Hz}$ was

achieved in the direct readout scheme without additional feedback circuitries. In this case, both the flux-to-voltage transfer coefficient $\partial V/\partial \Phi$ and the SQUID intrinsic $\delta \Phi_s$ increased. In other words, a compromise between $\delta \Phi_s$ and the noise contribution of preamplifier $\delta \Phi_{preamp}$ should be made for the weakly damped SQUIDs. It was found that SQUIDs with $\beta_c \approx 3$ can both exhibit an acceptable intrinsic noise $\delta \Phi_s$ and a sufficiently large $\partial V/\partial \Phi$ with respect to the voltage noise $V_n \approx 0.9$ nV/$\sqrt{\text{Hz}}$.

References

[1] Drung D and Mück M 2004 *SQUID Electronics: The SQUID Handbook* (Vol. 1) (Ed. Clarke J and Braginski A I) (Weinheim: Wiley-VCH) pp. 127–70

[2] Forgacs R L and Warnick A 1967 *Rev. Sci. Instrum.* **38** 214

[3] Drung D, Cantor R, Peters M, Scheer H J and Koch H 1990 *Appl. Phys. Lett.* **57** 406

[4] Seppä H, Ahonen A, Knuutila J, Simola J and Vilkman V 1991 *IEEE Trans. Magn.* **27** 2488

[5] Xie X, Zhang Y, Wang H, Wang Y, Mück M, Dong H, Krause H J, Braginski A I, Offenhäusser A and Jiang M 2010 *Supercond. Sci. Technol.* **23** 065016

[6] Wellstood F C, Urbina C and Clarke J 1987 *Appl. Phys. Lett.* **50** 772

[7] Schmelz M, Stolz R, Zakosarenko V, Schönau T, Anders S, Fritzsch L, Mück M and Meyer H G 2011 *Supercond. Sci. Technol.* **24** 065009

[8] Liu C, Zhang Y, Mück M, Krause H J, Braginski A I, Xie X, Offenhäusser A and Jiang M 2012 *Appl. Phys. Lett.* **101** 222602

[9] Zeng J, Zhang Y, Mück M, Krause H J, Braginski A I, Kong X, Xie X, Offenhäusser A and Jiang M 2013 *Appl. Phys. Lett.* **103** 042601

[10] Liu C, Zhang Y, Mück M, Zhang S, Krause H J Braginski A I, Zhang G, Wang Y, Kong X, Xie X, Offenhäusser A and Jiang M 2013 *Supercond. Sci. Technol.* **26** 065002

[11] Qiu Y, Liu C, Zhang S, Zhang G, Wang Y, Li H, Zeng J, Kong X and Xie X 2014 *Chin. Phys. B* **23** 088503

[12] Zhang Y, Liu C, Schmelz M, Krause H J, Braginski A I, Stolz R, Xie X, Meyer H G, Offenhäusser A and Jiang M 2012 *Supercond. Sci. Technol.* **25** 125007

[13] Zeng J, Zhang Y, Mück M, Krause H J, Braginski A I, Kong X, Xie X, Offenhäusser A and Jiang M 2013 *Appl. Phys. Lett.* **103** 122605

[14] Voss R F 1981 *J. Low Temp. Phys.* **42** 151

[15] Drung D and Jutzi W 1985 *IEEE Trans. Magn.* **21** 430